At the frontier between heterogeneous and homogeneous catalysis

Rangheard, Claudine; Julián Fernández, César de; Phua, Pim-Huat; Hoorn, Johan; Lefort, Laurent; Vries, Johannes G. de

Published in:
Dalton Transactions

DOI:
10.1039/c0dt00177e

Publication date:
2010

At the frontier between heterogeneous and homogeneous catalysis: hydrogenation of olefins and alkynes with soluble iron nanoparticles†

Claudine Rangheard,[a] César de Julián Fernández,[b] Pim-Huat Phua,[a] Johan Hoorn,[c] Laurent Lefort*[a] and Johannes G. de Vries*[a]

Received 19th March 2010, Accepted 30th July 2010
DOI: 10.1039/c0dt00177e

The use of non-supported Fe nanoparticles in the hydrogenation of unsaturated C–C bonds is a green catalytic concept at the frontier between homogeneous and heterogeneous catalysis. Iron nanoparticles can be obtained by reducing Fe salts with strong reductants in various solvents. $FeCl_3$ reduced by 3 equivalents of EtMgCl forms an active catalyst for the hydrogenation of a range of olefins and alkynes. Olefin hydrogenation is relatively fast at 5 bar using 5 mol% of catalyst. The catalyst is also active for terminal olefins and 1,1′ and 1,2-*cis* disubstituted olefins while *trans*-olefins react much slower. 1-Octyne is hydrogenated to mixtures of 1-octene and octane. Kinetic studies led us to propose a mechanism for this latter transformation where octane is obtained by two different pathways. Characterization of the nanoparticles *via* TEM, magnetic measurements and poisoning experiments were undertaken to understand the true nature of our catalyst.

Introduction

From an industrial point of view, hydrogenation catalysts based on iron are very attractive. Iron is abundant on earth and consequently its compounds are a few orders of magnitude cheaper than those of other metals more commonly used in hydrogenation such as Pd, Pt, Rh or Ir. Additionally, iron complexes are usually non-toxic and can be handled and disposed of easily. Currently there is a lot of renewed interest in the use of iron compounds as catalysts for various transformations.[1] However, outside the Fischer–Tropsch process[2] and the Haber–Bosch ammonia synthesis,[3] the use of iron in heterogeneous hydrogenation is rather limited. For the hydrogenation of unsaturated C–C bonds, there are only a few publications where high temperatures and pressures are used.[4] In addition, RANEY®-iron, Urushibara iron and iron metal obtained from the decomposition of $Fe(CO)_5$ were used for the hydrogenation of alkynes.[5] Examples of efficient homogeneous hydrogenation of C–C double or triple bonds with Fe complexes are also scarce.[6] Early trials focused on Ziegler–Natta type of catalysts where Fe salts were reduced by AlR_3.[7] In the 1970's, iron carbonyl complexes have been used as poorly active hydrogenation catalysts.[8] More recently, Fe complexes with phosphine[9] or imine[10] ligands have been used. The latter catalysts have not only shown high activities in the hydrogenation of simple alkenes, but also N– and O-containing olefins. Instead of searching for new ligands to impart hydrogenation activity to homogeneous Fe complexes, we decided to explore the use of soluble Fe nanoparticles. Our hope was that these peculiar entities at the frontier between homogeneous and heterogeneous could be intrinsically active in the hydrogenation of unsaturated C–C bonds. Soluble transition metal nanoparticles have attracted a lot of interest from the catalytic community in the last few decades.[11] Their activity is known to be very high under mild conditions because of their very large surface area compared to heterogeneous catalysts. An additional advantage is that they can be more easily recovered compared to truly homogeneous catalysts. Iron nanoparticles have already found use in a wide range of applications including magnetic fluids, catalysts for carbon nanotubes formation, magnetic resonance imaging (MRI) contrast agents, nickel–iron batteries, catalysts and sorbents for environmental remediation.[12] However, their use in catalysis has remained only marginal and centered on C–C formation reactions.[13] Additionally, we anticipated that Fe nanoparticles could be prepared *via* a simple procedure with cheap stabilizers or even without stabilizers, thus warranting an extremely cost-efficient catalyst.

In an earlier communication, we reported the synthesis of soluble Fe–NPs prepared *via* Grignard reduction and their use in the hydrogenation of olefins and alkynes.[14] In this article, we present a systematic study aimed at understanding how the method of NPs synthesis as well as the hydrogenation conditions affect the catalytic activity of nanoparticles. Kinetic studies during the alkyne hydrogenation led us to propose a mechanism. Characterization of the nanoparticles by TEM, magnetic measurements, and chemical poisoning experiments are presented.

Results and discussion

Synthesis of the Fe nanoparticles and their catalytic activity

A number of synthetic methods for the preparation of Fe nanoparticles (Fe–NPs) have been reported,[12g] such as the thermal decomposition of iron carbonyl complexes,[15] the hydrogenation of iron amides[16] and the chemical reduction of iron salts.[17] In our first trials, we decided to use this last method. Using our high

[a]*DSM Innovative Synthesis B.V., a unit of DSM Pharma Chemicals, P. O. Box 18, 6160, MD Geleen, The Netherlands*
[b]*Laboratorio di Magnetismo Molecolare, INSTM - Dipartimento di Chimica, Università degli Studi di Firenze, Polo Scientifico - Via della Lastruccia 3, 50019, Sesto Fiorentino (FI), Italy*
[c]*DSM Advanced Chemical Engineering Solutions, P. O. Box 18, 6160, MD Geleen, The Netherlands*

† Electronic supplementary information (ESI) available: Additional experimental details. See DOI: 10.1039/c0dt00177e

Table 1 Influence of the reducing agent in the hydrogenation activity[a]

Entry	Reducing agent	Conversion norbornene (%)
1	Me_3Al	0
2	Et_3Al	50
3	MeLi	100
4	*n*-BuLi	100
5	PhLi	100
6	MeMgCl	100
7	EtMgCl	100
8	*i*-PrMgCl	100
9	PhMgBr	100
10	EtMgCl (1 eq/Fe)	0
11	EtMgCl (2 eq/Fe)	0
12	EtMgCl (4 eq/Fe)	100

[a] Conditions: Reduction Fe salt: $FeCl_3$ (0.05 mmol), 3 eq. reducing agent, THF (1 mL), R.T., 15 min; Hydrogenation: norbornene (1 mmol), THF (3 mL), R.T., 10 bar H_2, 30 min.

Table 2 Influence of the iron precursor on the hydrogenation activity[a]

Entry	Iron precursor	EtMgCl (eq/Fe)	Conversion norbornene (%)
1	$FeCl_3$	3	100
2	$Fe(acac)_3$	3	100
3	$FeCl_2$	3	100
4	$FeCl_2$	2	70
5	FeI_2	3	100
6	FeI_2	2	100
7	$Fe(OAc)_2$	3	100
8	$Fe(OAc)_2$	2	100

[a] Conditions: Reduction Fe salt: Fe salt (0.05 mmol), reducing agent, THF (1 mL), R.T., 15 min; Hydrogenation: norbornene (1 mmol), THF (3 mL), R.T., 10 bar H_2, 30 min).

throughput experimentation equipment,[18] we were able to quickly test a wide range of Fe salts ($FeCl_3$, $Fe(Acac)_3$, $Fe(NO_3)_3$, $Fe(SO_4)$, $FeCl_2$, $FeBr_2$, FeI_2, $Fe(OAc)_2$) in combination with 11 different stabilizers (PEG, PVP, SDS, primary amines, ammonium bromide) reduced by $NaBH_4$ in EtOH. The resulting Fe species were tested in the hydrogenation of norbornene at 80 °C under 20 bar of H_2. Most of the combinations did not show any hydrogenation activity. Only when using FeI_2 or $FeCl_2$, small amounts of norbornane were detected but the results were difficult to reproduce on larger scale. In 2006, during a study on the coupling of alkyl halides with aryl magnesium bromides with Fe complexes, Bedford *et al.* noticed that independently of the homogeneous Fe catalysts used, the reaction mixture would immediately turned black upon addition of the Grignard reagent. A transmission electron microscopy image of the reaction mixture revealed the presence of Fe–NPs thus pointing towards a new method for the preparation of Fe–NPs, *i.e.* the reduction of Fe halides with a Grignard reagent.[13a] Immediately after the discovery of the Ziegler–Natta catalyst in the 1960's, several groups studied the reaction of Fe salts with AlR_3 and other "alkylating" agents[19] and some even tested the activity of the obtained Fe species in hydrogenation.[7,20] However, none of these reports clearly mention the presence of Fe–NPs. Identically, Fe complexes were extensively used in cross-coupling reaction where they were contacted with Grignard and other alkylating reagents.[1a,21] Currently, there is no definitive consensus on the mechanism of this transformation where catalytic cycles involving Fe(+I)/Fe(+III),[22] Fe(0)/Fe(+II)[22a,23] or even Fe(-II)/Fe(0)[24] have been proposed. Considering our initial goals to test Fe nanoparticles in hydrogenation, the recent report of Bedford, and the early successes met with Ziegler–Natta type catalysts in hydrogenation, we decided to switch from $NaBH_4$ to other reductants.

The reduction of $FeCl_3$ was carried using different reducing agents such as trialkyl aluminiums, alkyl lithiums, Grignard reagents, tetraalkyllead and tetraalkyltin. The reactions were performed using 3 equivalents of reducing agents in THF under inert atmosphere. In most cases, the color of the solution changed instantaneously from yellow to dark brown/black. The supposedly obtained Fe–NPs were tested in norbornene hydrogenation (Table 1).

Gratifyingly, many reducing agents convert $FeCl_3$ into an active catalyst for the hydrogenation of norbornene (Table 1). All lithium and Grignards reagents allowed the formation of a catalyst giving full conversion of the norbornene to norbornane. We observed a remarkable difference between $AlMe_3$ (Entry 1) and $AlEt_3$ (Entry 2) although the same dichotomy was not observed for the Grignard reagents (Entry 6,7). Fürstner published a proposal regarding the mechanism of the reduction of iron chloride salts by EtMgBr based on the observation of released ethane and ethylene.[24] He reports a difference of reactivity in cross-coupling reactions between methyl and ethyl alkylating agents.[18] In agreement with the observations of Bogdanović,[25] he attributes this difference to the possibility (with EtLi or EtMgCl) or impossibility (with MeLi or MeMgCl) for the metal to undergo β-hydride elimination in its reduction process. We do not observe such a difference as both MeLi and MeMgCl as well as PhMgBr lead to an active catalyst. In the case of EtMgCl, the effect of the ratio of Grignard reagent relative to Fe was probed. Using 2 equivalents of Grignard reagents or less, no hydrogenation activity was obtained while 3 equivalents or more give full conversion. This minimum ratio EtMgCl : Fe of 3 : 1 is consistent with the reduction of Fe(+III) into Fe(0). In a set of control experiments, $MgCl_2$, EtMgCl, EtMgCl/$MgCl_2$ and $FeCl_3$/$MgCl_2$ were tested in hydrogenation. In all cases, no hydrogenated product was observed. At this stage, we decided to use EtMgCl as the standard reducing agent in the rest of our study.

We then investigated the influence of the iron precursors on the activity of the Fe–Np's. Five different Fe salts were reduced by EtMgCl in THF and then tested in norbornene hydrogenation (Table 2). $FeCl_3$ and $Fe(acac)_3$ are entirely soluble in THF while the other iron salts $FeCl_2$, FeI_2 and $Fe(OAc)_2$ are not. After addition of EtMgCl, all the reaction mixtures turned black and no remaining solid material was present. In contrast to $FeCl_3$, a ratio EtMgCl : Fe of 2 : 1 was sufficient to prepare an active catalyst from Fe(+II) precursors (Entries 4,6). This is again in agreement with the reduction of Fe(+II) into Fe(0). $FeCl_3$ was chosen as our standard iron precursor due to its high solubility in THF.

Various solvents (tetrahydrofuran, toluene, heptane, dioxane, ethyl acetate, diethylether) were tested for the preparation of the catalyst. $FeCl_3$ is entirely soluble in tetrahydrofuran, dioxane, ethylacetate and diethylether, but only partially soluble in toluene and heptanes at [Fe] = 0.05 M (see supplementary information†). Upon treatment with 3 eq. of EtMgCl, all the solutions turned instantaneously brown/black. Formation of a deposit occurred overnight in all solvents except for toluene and THF. However, full conversion to norbornane (Reaction conditions: 5 mol% Fe–NPs, [Alkene] = 0.33 M, 3 mL solvent, 10 bar H_2, R.T.) was

nevertheless obtained in all solvents except in EtOAc and heptane. Interestingly, the Fe–NPs prepared in THF could be dried and entirely redispersed in the same solvent.

As already reported,[14] the $FeCl_3$/EtMgCl system is active in the hydrogenation of a range of olefins (Fig. 1) and alkynes. Aliphatic linear terminal, *gem*-disubstituted and linear *cis*-olefin are fully converted. Cyclic olefins lacking cycle strain and *trans*-olefins are more difficult to hydrogenate and require higher temperature to give full conversion. More bulky substrates such as tri- and tetrasubstituted olefins were not hydrogenated even at 100 °C. Equally, no reaction was observed towards anisole, nitrobenzene, acrylate and amido-acrylate. In the latter two cases, this may be due to the incompatibility of our catalyst with esters as already indicated by its low activity in EtOAc. Here, we decided to monitor the progress of the 1-octyne hydrogenation reaction over a period of a few hours in order to gain more insight into the selectivity. Three experiments with different settings were performed in an autoclave at 40 °C under 5 bar of hydrogen (Fig. 2 to 4). Under the reaction conditions only the hydrogenated products, *i.e.* 1-octene and n-octane were formed and no by-products were observed.

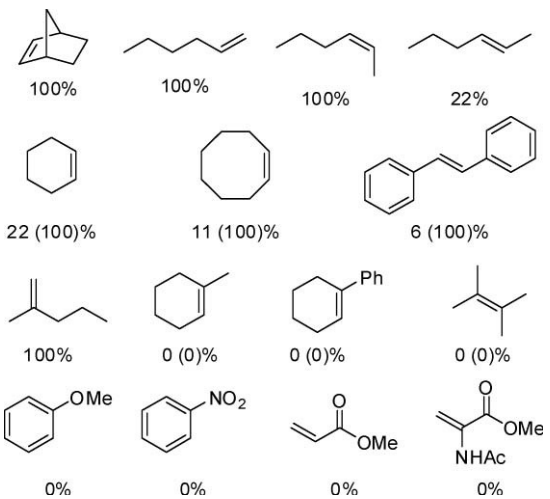

Fig. 1 Scope of the $FeCl_3$/EtMgCl hydrogenation catalyst (Reaction conditions: 5 mol% Fe, [Alkene] = 0.33 M, THF, 20 bar H_2, R.T. except values in parentheses at 100 °C, 18 h).

As can be seen from Fig. 2, the catalyst becomes active 10 min after the introduction of H_2. The reason for this induction period remains unclear. At this point, the reaction order in 1-octyne follows zero-order behavior. The formation of n-octane and 1-octene from 1-octyne is simultaneous and the ratio of their respective rates is constant. When all 1-octyne has reacted, the hydrogenation of 1-octene proceeds much faster and appears to be first order in 1-octene.[26] This suggests that the active sites of the catalyst are predominantly occupied by the alkyne, thus retarding the hydrogenation of 1-octene. Consequently, in the presence of 1-octyne, 1-octene is prevented from binding to the catalyst and the initially observed n-octane must be produced *via* direct hydrogenation of 1-octyne without release and re-adsorption of 1-octene.

At a lower catalyst concentration, the rate of 1-octyne disappearance is reduced but the reaction order appears to be also zero (Fig. 3). The ratio of the formation rates of 1-octene and n-octane

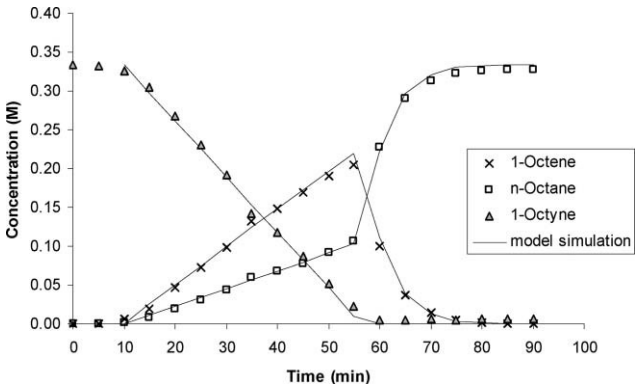

Fig. 2 Concentration 1-octyne, 1-octene and n-octane *vs.* time at high catalyst concentration (Reaction conditions: 0.9 g l^{-1} Fe (0.017 M), [1-Octyne] = 0.33 M, THF, 5 bar H_2, 40 °C).

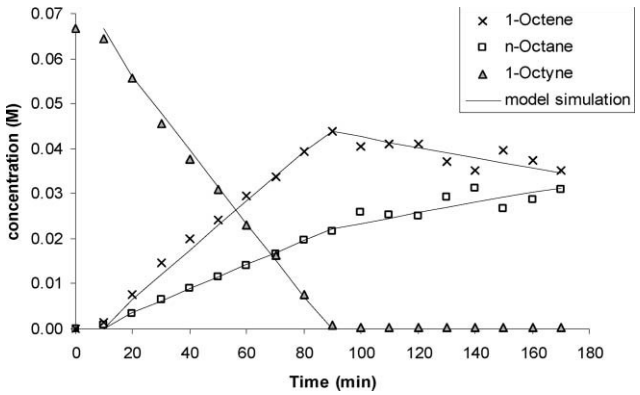

Fig. 3 Concentration 1-octyne, 1-octene and n-octane *vs.* time at low catalyst concentration (Reaction conditions: 0.2 g l^{-1} Fe (0.0034 M), [1-Octyne] = 0.067 M, THF, 5 bar H_2, 40 °C).

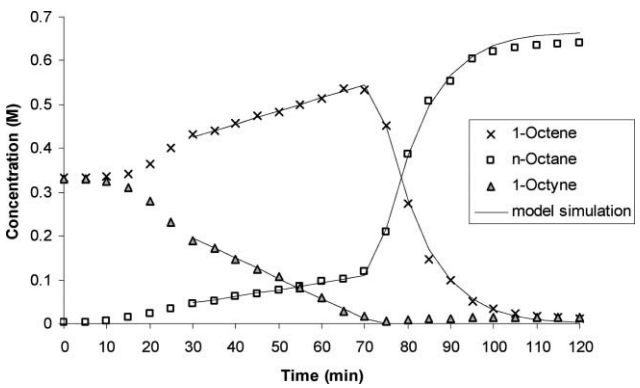

Fig. 4 Concentration 1-octyne, 1-octene and n-octane *vs.* time starting with 1-octyne and 1-octene simultaneously (Reaction conditions: 0.9 g l^{-1} Fe (0.017 M), [1-Octyne] = 0.33 M, [1-Octene] = 0.33 M, THF, 5 bar H_2, 40 °C).

is also constant when 1-octyne is still present. Interestingly, the rate of hydrogenation of 1-octene after complete consumption of 1-octyne is much more affected by the lower concentrations used in this experiment, becoming even slower than the rate of hydrogenation of 1-octyne. This behaviour is consistent with the proposed orders of reactions, *i.e.* 0 for the alkyne hydrogenation and 1 for the alkene hydrogenation.

Next to the experiments, a simple Langmuir-Hinselwood type model was developed (see supplementary information) to verify some of the hypotheses regarding the mechanism. For all experiments the initial induction periods were not included in the data used to tune the model as the start-up phenomena were too complicated to be described by a simple model. A good fit between the model and the experimental data could be obtained only if the equilibrium constant for the reversible binding of 1-octyne to the catalyst is set to be 10^4 higher than for 1-octene (see curves on Fig. 2 and 3). Further corroboration of this was obtained by an experiment in which we hydrogenated 1-octyne in the presence of 1-octene.

When the hydrogenation was performed with an equal concentration of 1-octyne and 1-octene, the induction period was slightly longer than in the absence of 1-octene (Fig. 4). During this period, a small amount of 1-octene hydrogenation also appears to take place as the initial formation rate of n-octane is slightly higher than the disappearance rate of 1-octyne. However, after 30 min 1-octyne hydrogenation completely dominates and no conversion of 1-octene is found as long as 1-octyne is present. When 1-octyne is completely converted the hydrogenation rate of 1-octene is equal to the experiment with similar catalyst concentration (Fig. 2).

We propose that in the presence of 1-octyne, the initially observed n-octane must be produced *via* direct hydrogenation of 1-octyne without release and re-adsorption of 1-octene. A possible mechanism for this transformation is depicted in Scheme 1. After exposure to H_2, the Fe–NPs have formed either some hydrides and/or some dihydrogen species. The presence of hydrogen on the Fe–NPs was proven by H_2 titration experiments (2.5 hydrogen atom per exposed iron atom), which we describe later in this article. However, the exact binding mode of the hydrogen atoms is unknown at this stage. For convenience, we write a mixed hydride-dihydrogen species (**1**) based on the mechanism decribed by Bianchini and Oro for alkyne hydrogenation with a homogeneous iron complex.[9a] We assume that insertion of the alkyne into the Fe–H bond occurs leading to a Fe-alkenyl complex (**2**) that forms 1-octene *via* reductive elimination (Path 1). Additionally, we can also imagine that in the presence of H_2, intermediate (**2**) rearranges to form an iron hydride alkylidene (**3**).[27] Such iron carbenes, which in some instances are formed by reaction of Fe complexes with alkynes are known.[28] The Fe alkylidene can be hydrogenated to an iron alkyl compound (**4**). Upon further reaction with H_2, the latter compound forms n-octane and regenerates the starting Fe species.

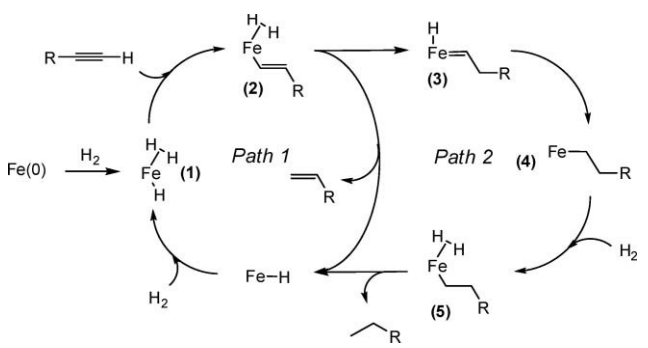

Scheme 1 Proposed mechanism for the direct hydrogenation of 1-octyne to n-octane (Fe denotes an iron atom at the surface of the nanoparticles).

Table 3 Selectivities of the bimetallic catalyst in 1-octyne hydrogenation[a]

Entry	Metal nanoparticles	1-Octene : Octane
1	Fe	1 : 0.42
2	Ni	1 : 0.16
3	Co	1 : 0.32
4	Cu	No activity
5	Fe : Ni (1 : 1)	1 : 0.26
6	Fe : Co (1 : 1)	1 : 0.34
7	Fe : Cu (1 : 1)	No activity

[a] Reaction conditions: 5 mol % metal, [1-Octyne] = 0.33 M, THF, 5 bar H_2, R.T.

The induction period observed in the initial phase can be caused by a number of reasons. One possible explanation would be a further decrease in size of the nanoparticles either by binding to the substrate or to hydrogen. Gates observed that supported iridium clusters decrease in size upon addition of alkenes.[29] Ageing the Fe–NPs in presence of 1-octyne slightly increases their activity (see supplementary information, Figure S3†). Additionally, ageing the nanoparticles in absence of 1-octyne also changes their activities but in this case, different behaviours are obtained depending on the concentration of the $FeCl_3$ solution used to prepare the nanoparticles. TEM measurements after the different treatments of the nanoparticles could help to establish an eventual structure–activity relationship.

In order to suppress the hypothetic direct pathway to octane, we decided to turn towards bimetallic nanoparticles. Selective poisoning of some of the active sites of a catalyst by a second metal is a common method to improve the selectivity. Our bimetallic nanoparticles were prepared by adding a second cheap metal halide ($NiCl_2$, $CoCl_2$, $CuCl_2$) to $FeCl_3$ in a 1 : 1 ratio and reducing both metals with 3 eq of EtMgCl. The resulting bimetallic catalysts were tested in the hydrogenation of 1-octyne (Fig. 5 for activities; Table 3 for selectivities).

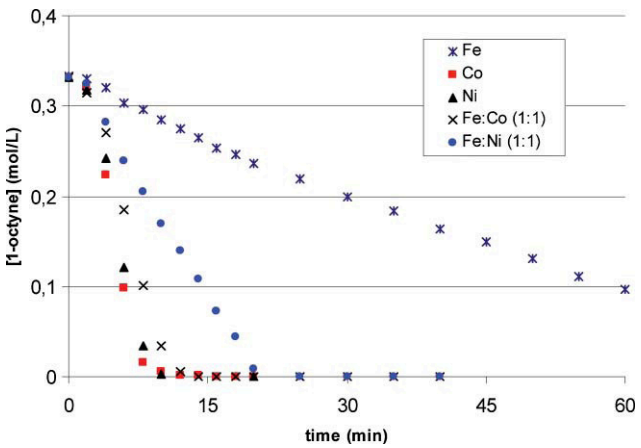

Fig. 5 Concentration of 1-octyne *vs.* time for various monometallic and bimetallic catalysts (Reaction conditions: 5 mol % total metal content, [1-Octyne] = 0.33 M, THF, 5 bar H_2, R.T.).

As can be seen in Fig. 5, the monometallic Ni and Co nanoparticles are much more active towards 1-octyne hydrogenation than Fe–NPs. Cu–NPs and Fe–Cu NPs (prepared from $CuCl_2$, not shown) are inactive in our reaction conditions. Bimetallic Fe–Co–NPs have almost the same activity as Co-NPs while Fe–Ni-NPs

display an intermediate activity between both single metal NPs. As long as 1-octyne is present, the ratio 1-octene:octane stays constant as already observed for Fe–NPs. Both active bimetallic catalysts (FeNi, FeCo) exhibit intermediate selectivities compared to the corresponding monometallic components (Table 3). These are promising first results that show that the selectivity of the hydrogenation can be modified using polymetallic NPs.

Characterization of the Fe catalyst

Having prepared an active hydrogenation catalyst based on Fe, we then decided to proceed with its characterization and the identification of the active Fe species. As already reported,[14] transmission electron microscopy of a solution of $FeCl_3$ treated with EtMgCl confirmed the presence of Fe nanoparticles (NPs) with an average size of 2.67 ± 0.60 nm (Fig. 6).

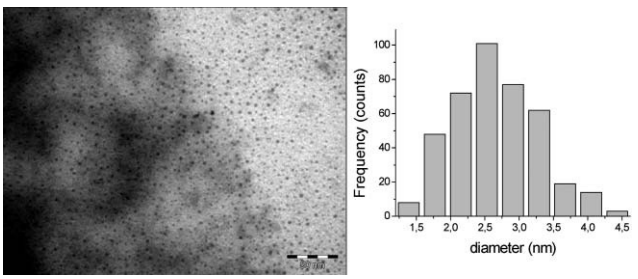

Fig. 6 TEM micrographs of Fe nanoparticles obtained from $FeCl_3$/EtMgCl.

Unsurprisingly, EDX showed that the solids are composed of iron, magnesium and chlorine. Although we do not use a stabilizer, visual inspection of our Fe–NPs after 1 night in THF does not reveal any precipitate. We assume that $MgCl_2$ and possibly THF act as stabilizer. Finke[30] recently reported that even BF_4^- is a better stabilizer of NPs than ethereal solvents. It thus seems highly likely that the chloride ions of $MgCl_2$ will bind to the outer rim of the Fe–NPs. In order to probe the influence of $MgCl_2$ on the activity of the catalyst in hydrogenation, we added various amounts (from 0.5 to 20 eq/Fe) of anhydrous $MgCl_2$ to freshly prepared Fe–NPs and tested their activity in the hydrogenation of norbornene in the standard reaction conditions (R.T., 10 bar H_2, 30 min). No influence of added $MgCl_2$ was observed since in all cases, norbornene was fully converted to norbornane. Advantageously, if $MgCl_2$ is effectively acting as a stabilizer, even an excess of it does not prevent the substrate from reaching the active site of the catalyst as is sometimes the case with more traditional stabilizers.

To further characterize the Fe–NPs, their magnetic properties were measured using a Quantum Design superconducting quantum interference device (SQUID) magnetometer. In Fig. 7a, the hysteresis loops, in terms of magnetization per gram of Fe, measured at 3 K and 40 K are represented. The density of magnetization reached at 3 K is 224 ± 5 emu/gr, value in excellent accordance with the one of bulk bcc Fe(0), 220 emu/gr.[31] The presence of iron oxides is excluded as their magnetizations, in the best of the cases (for magnetite and maghemite), are less than half this value.[31] Moreover the value of the magnetization above 20 kOe is well saturated. This excludes nanostructural features like the presence of ions and/or oxide nanoparticles with the uncompensation of the antiferromagnetic order or size-

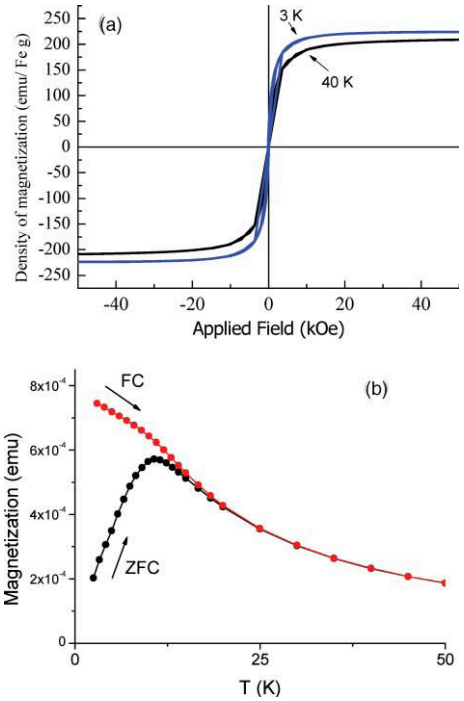

Fig. 7 (a) Hysteresis loops measured at the temperature of 3 K and 40 K; (b) temperature dependence of the Zero-field-cooling and field cooling magnetizations.

effects[32] that give rise to the non-saturation of the field dependent magnetization. These two results indicate the exclusive grown of metallic Fe nanoparticles. The large magnetic moment in nanoparticles is one desirable property for many applications but often the magnetic moment is smaller due to oxidation of the surface or to the chemical interaction with the capping agent. Free Fe clusters with similar or smaller sizes than 2–3 nm[33] exhibit even higher magnetizations but their transfer to physical or chemical supports is difficult. Bulk like magnetizations were also observed by Chaudret *et al.*[34] in Fe capped nanoparticles synthesized by hydrogenation of $Fe[N(SiMe_3)_2]_2$ but the average particle size is larger (7 nm).

Fig. 7a also shows that at low temperatures K the hysteresis loop exhibits both coercive field (150 Oe) and magnetization at zero field (remanence) while at 40 K these properties are zero. This change of magnetic behavior is a consequence of thermal demagnetization effects. At low temperatures, the magnetic state is defined as blocked while at higher temperatures the nanoparticles exhibits superparamagnetism behaviour.[35] The temperature dependence of the ZFC magnetization exhibits a maximum at 10 K (Fig. 7b) corresponding to the temperature at which most nanoparticles change from blocked to superparamagnetic. Moreover above 20 K, the temperature at which the FC curve joins the ZFC curve, all the nanoparticles are superparamagnetic. The change from the blocking regime to the superparamagnetic regime is an additional evidence of the nanometric nature of the particles. Because of their small size, the thermally driven demagnetization leads to a relaxation process occurring faster than the measurement time. The description of this relaxation time in terms of the Arrhenius expression[35,36] for this type of materials and for the SQUID measurements is given by the following expression: $25\ k_B T_B = K_{ef} \cdot V_m$, where T_B is the blocking temperature, V_m the average

particle volume, K_{ef} the effective magnetic anisotropy, k_B the Boltzmann constant. K_{ef} is equal to 2×10^6 ergcm^{-3} if V_m is 19 nm^3 (considering the lognormal distribution from the TEM histogram) and $T_B = 11$ K. The K_{ef} value is larger than the one of bulk bcc Fe[36] indicating an enhancement of the anisotropy. Such an effect can be due either to the local enhancement of the spin–orbit coupling caused by the breaking of the crystalline symmetry at the surface of the nanoparticles[32c,33] or to the electronic localization in some surface Fe–Cl bonds.

Although TEM and magnetic measurements showed the presence of nanoparticles, one can not exclude that the active hydrogenation species are molecular Fe complexes. Selective poisoning tests are commonly used to identify the nature of the true catalyst.[37] Hg is a well known poison for nanoparticles due to the formation of an amalgam while the molecular metal complexes remains unaltered. This property of Hg was first exploited by Whitesides and co-workers.[38] The experiment consists in adding Hg(0) to the reaction mixture and the suppression of catalytic activity is a strong evidence for catalysis by nanoparticles. In our case, the conversion of norbornene to norbornane was reduced to 40% instead of 100% when the hydrogenation was performed with Fe–NPs that had been vigorously stirred for 1 h with Hg(0). This intermediate result is inconclusive. However, one report mentions that iron may not form a stable alloy with Hg(0)[39] which could explain the residual activity. Another poisoning study consists in using ligands that strongly bind to a metal center such as thiophene and triphenylphosphine that can block access of the substrate to the active site. If a catalyst can be poisoned by a sub-stoichiometric amount of poison ($\ll$1eq per metal atom), it can be concluded that the true catalyst are nanoparticles since in this case, only a fraction of the metal atoms, *i.e.* the ones on the surface, are active. On the other hand if the catalyst is poisoned with one or more equivalent of poisoning ligands, it is generally concluded that the catalyst is a homogeneous metal complex. In our case, thiophene or PPh_3 (0.1–1 eq/Fe with PPh_3, 0.1–5 eq/Fe with thiophene) did not alter the activity of our system in norbornene hydrogenation. Sulfur containing substrates are notoriously difficult to hydrogenate with most heterogeneous catalysts. Even homogeneous catalysts are seriously retarded by the presence of thioethers.[40] Consequently, we took advantage of this last result and demonstrated that our Fe catalyst is able to hydrogenate a sulfur containing olefin, *i.e.* 2-allyl-thiophene. Using 5 mol% of Fe–NPs in THF, at R.T. and 10 bar of H_2, this substrate was fully hydrogenated after 30 min. We are currently testing our catalyst with other S- and P-containing substrates.

To a certain extent, our Fe–NPs were also remarkably resistant towards protic additives. The catalyst was pretreated with various amount of degassed H_2O during 15 min prior to the hydrogenation (Fig. 8). Up to 50 equivalents of H_2O/Fe are necessary to completely eliminate the activity of the catalyst in norbornene hydrogenation. The same holds true with the less protic MeOH. An explanation for this behavior may be that highly hygroscopic $MgCl_2$ may scavenge H_2O and protect to a certain extent Fe(0) from oxidation. Only two equivalents of acetic acid are necessary to completely deactivate the catalyst. In this case, the brown/black solution of Fe–NPs becomes quickly yellow corresponding to the redissolution of the Fe(0) species as iron acetate species.

Following the methodology described by Chaudret *et al.*,[41] we investigated the presence of hydrogen or hydrides on the surface of

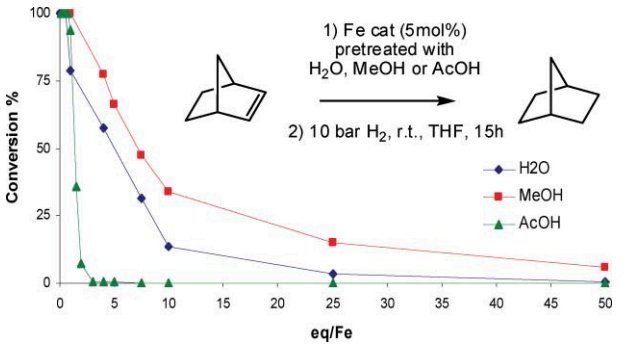

Fig. 8 Influence of protic additives in the hydrogenation activity of the Fe catalyst.

our Fe nanoparticles. In these experiments, the nanoparticles are first exposed to 10 bar of hydrogen for 1 h at room temperature. After removal of H_2, an atmosphere of nitrogen is introduced (three cycles of high pressure nitrogen followed by a purge), norbornene is added to the Fe nanoparticles and the amount of norbornane is determined by gas chromatography. Different amounts of Fe nanoparticles (0.0125 to 0.175 mmol Fe) were contacted with the same amount of norbornene (0.1 mmol). The amount of norbornane obtained *vs.* the amount of Fe is plotted in Fig. 9. The slope of the straight line fitting the experimental points is 0.46, indicating that there is about 1 H per total atoms of Fe. Assuming that our nanoparticles are monodispersed with an average diameter of 2.7 nm as measured by TEM, we can approximate the amount of H per atom of Fe on the surface to 2.45 or about 5 H per 2 atoms of Fe. To account for this odd number, one can assume the presence of a bridging H.

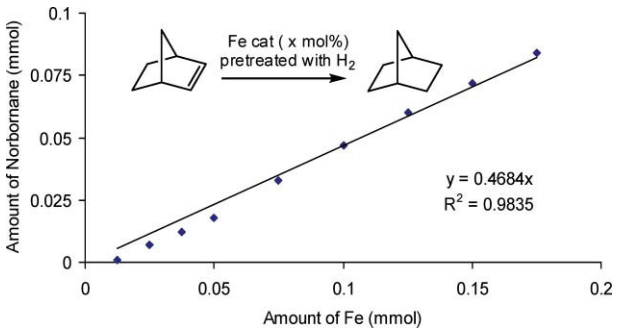

Fig. 9 Determination of the amount of H/H_2 in the catalyst.

Conclusion

We have shown that iron nanoparticles, prepared *via* reduction of iron salts in THF with alkyl Grignards or alkyl lithiums are good catalysts for the hydrogenation of alkenes and alkynes. A substrate containing a thioether was hydrogenated without any retardation. Kinetic measurements of the octyne hydrogenation led to the interesting observation that the alkyne binds much stronger to the surface of the iron nanoparticles than the alkene, leading us to propose a mechanism where alkane formed during the first phase of the hydrogenation when alkyne is still present is not caused by hydrogenation of alkene but rather results from an isomerisation of the initial formed alkenyl iron compound to an alkylidene iron compound, which is further hydrogenated to the alkane. Although

the presence of Fe(0) nanoparticles was proven by TEM, EDX and by magnetic measurements, we are still unable to ascertain whether they are the true active species in hydrogenation. We are currently pursuing the further characterization of the Fe–NPs and are extending their use to the hydrogenation of more challenging substrates.

Experimental procedures

General procedures

All manipulations were performed under a nitrogen atmosphere in an M. Braun glove box. Anhydrous solvents (THF, toluene, heptanes, ethyl acetate, DCM) from the M. Braun Solvent Purification System were used. The compounds 1-octyne, norbornene and the other substrates were obtained from Aldrich and used as received. Premex A 96 reactor (small scale reaction) and Parr autoclave (large scale reaction) were used for hydrogenation reactions. GC were performed on a Hewlett-Packard 5890 Gas Chromatography Series II using a CP-Sil-5CB Chrompack capillary column (50 m × 0.32 mm × 1.2 μm) or CP-Sil-5CB Chrompack capillary column (25 m × 0.25 mm × 0.25 μm). Transmission electron microscopy coupled with EDX (Energy Dispersive X-ray Spectrometer) was performed at Paul Sabatier University of Toulouse. The magnetic properties of the iron nanoparticles in THF were measured using a Quantum Design superconducting quantum interference device (SQUID) magnetometer at Laboratorio di Magnetismo Molecolare, INSTM, Firenze. The samples were placed into the magnetometer under inert atmosphere 5 min after their synthesis. Temperature-dependent zero-field-cooled (ZFC) and field-cooled (FC) magnetization measurements were obtained for a range of temperatures between 2.5 K and 140 K (below the melting point of the THF) with an applied magnetic field of 10 Oe. The hysteresis loops were recorded at 3 K and at 40 K for a maximum applied magnetic field of 50 kOe. The dia and paramagnetic contributions of the sample holder and THF were measured and subtracted to the measurement. The density of magnetization was calculated considering the amount of iron in the synthesis.

Standard procedure to prepare Fe-NPs from $FeCl_3$ and EtMgCl

In the N_2 glovebox, $FeCl_3$ (0.1622 g, 1.0 mmol) was dissolved in dry THF (20.0 mL). A 2.0 M solution of EtMgCl (2.50 mL) in THF was added *via* syringe. The reaction mixture turns instantaneously from yellow to brown/black. The reaction mixture was vigorously stirred for 30 min. Iron nanoparticles were used without further purification. The synthesized catalyst was characterized by transmission electron microscopy coupled with EDX (Energy Dispersive X-ray Spectrometer) and magnetic measurements using a Quantum Design superconducting quantum interference device (SQUID) magnetometer.

Hydrogenation of alkenes or alkynes (substrate screening)

To a 5 mL reaction vial containing a stirring bar, an alkene or an alkyne (1.0 mmol) in THF (1.0 mL) was added. 1.0 mL of the catalyst solution (a) prepared as described above (1.0 mL, [Fe] = 0.05 M, S/C = 20) was added to the reaction mixture under nitrogen. The reaction mixture was then vigorously stirred in the presence of hydrogen at 20bar at room temperature for 18 h in the Premex A96 Reactor. The hydrogenated products were then analyzed by GC.

Hydrogenation of 1-octyne in the autoclave

In the glovebox, 1-octyne (2.57 g, 23.3 mmol) and THF (44.5 mL) were added to a 150 ml Parr autoclave. 23.5 mL of the catalyst solution (0.05 M), prepared from 0.138 g of $FeCl_3$ (189.3 mg, 1.17 mmol) and EtMgCl (1,76 ml of a 2.0 M solution) in THF was added at once (S/C = 20). The vessel was purged 3 times with nitrogen and 3 times with hydrogen and kept under 5 bar of hydrogen at 40 °C under mechanical stirring at 800 rpm for 4 h. Samples were taken every 5 or 10 min and the hydrogenation products were analyzed by GC.

Acknowledgements

We thank the European Union for its financial support of this research which was carried out as part of the Research Training Network (R)evolutionary Catalysis (MRTN-CT-2006 035866).

References

1 (*a*) W. M. Czaplik, M. Mayer, J. Cvengroš and A. J. von Wangelin, *ChemSusChem*, 2009, **2**, 396; (*b*) B. D. Sherry and A. Fürstner, *Acc. Chem. Res.*, 2008, **41**, 1500; (*c*) C. Bolm, J. Legros, J. Le Paih and L. Zani, *Chem. Rev.*, 2004, **104**, 6217; (*d*) A. Fürstner and R. Martin, *Chem. Lett.*, 2005, **34**, 624; (*e*) A. Correa, O. G. Mancheno and C. Bolm, *Chem. Soc. Rev.*, 2008, **37**, 1108.
2 R. Schlögl, *Angew. Chem., Int. Ed.*, 2003, **42**, 2004.
3 W. Arabczyk, I. Jasinska and R. Jedrzejewski, *Catal. Commun.*, 2009, **10**, 1821.
4 (*a*) Z. Lu, C. Wang, D. Liang and L. Lin, *Shiyou Huagong*, 1991, **20**, 454; (*b*) Y. Nitta, S. Matsugi and T. Imanaka, *Chem. Express*, 1989, **4**, 547; (*c*) Y. M. Bondarev, Y. S. Mardashev, A. D. Mokrushin, V. F. Blokhin and I. V. Razumovskaya, *Zh. Fiz. Khim.*, 1985, **59**, 2343.
5 (*a*) S. Nishimura in *Handbook of Heterogeneous Catalytic Hydrogenation for Organic Synthesis*, J. Wiley & Sons, Inc., 2001, pp. 165 and references within; (*b*) A. F. Thompson, Jr. and S. B. Wyatt, *J. Am. Chem. Soc.*, 1940, **62**, 2555; (*c*) R. Paul and G. Hilly, *Bull. Soc. Chim.*, 1939, **6**, 218.
6 S. Enthaler, K. Junge and M. Beller in *Iron catalysis in Organic Chemistry. Reactions and applications*, ed. B. Plietker, Wiley-VCH, Weinheim, 2008, pp. 129-136 and references within.
7 (*a*) M. F. Sloan, A. S. Matlack and D. S. Breslow, *J. Am. Chem. Soc.*, 1963, **85**, 4014; (*b*) Y. Takegami, T. Ueno and T. Fujii, *Bull. Chem. Soc. Jpn.*, 1965, **38**, 1279; (*c*) N. F. Noskova, A. Zh. Kazimova, K. K. Kambarova, S. R. Savelév and N. L. Melamud, *Zh. Org. Khim.*, 1992, **28**, 1352.
8 (*a*) B. R. James, *Homogeneous Hydrogenation*, John Wiley & Sons, New York, 1973, pp. 64–72; (*b*) C. U. Pittman Jr., R. C. Ryan, J. McGee and J. P. O'Connor, *J. Organomet. Chem.*, 1979, **178**, C43; (*c*) M. A. Schroeder and M. S. Wrighton, *J. Am. Chem. Soc.*, 1976, **98**(2), 551; (*d*) Y. Tajima and E. Kunioka, *J. Org. Chem.*, 1968, **33**, 1689.
9 (*a*) C. Bianchini, A. Meli, M. Peruzzini, P. Frediani, C. Bohanna, M. A. Esteruelas and L. A. Oro, *Organometallics*, 1992, **11**, 138; (*b*) E. J. Daida and J. C. Peters, *Inorg. Chem.*, 2004, **43**, 7474.
10 (*a*) Q. Knijnenburg, A. D. Horton, H. Van der Heijden, A. W. Gal and P. H. M. Budzelaar, to *Stichting voor de Technische Wetenschappen*, Int. Pat. Appl., WO03042131, 2003; (*b*) S. C. Bart, E. Lobkovsky and P. J. Chirik, *J. Am. Chem. Soc.*, 2004, **126**, 13794; (*c*) R. J. Trovitch, E. Lobkovsky, E. Bill and P. J. Chirik, *Organometallics*, 2008, **27**, 1470.
11 (*a*) A. Roucoux and K. Philippot, in *Handbook of Homogeneous Hydrogenation*, ed. J. G. de Vries and C. J. Elsevier, Wiley-VCH, Weinheim, 2007, vol. 1, pp. 217-256; (*b*) A. Roucoux, A. Nowicki and K. Philippot, in *Nanoparticles in Catalysis*, ed. D. Astruc, Wiley-VCH, Weinheim, 2008, pp. 349-388; (*c*) D. Astruc, F. Lu and J. Ruiz Aranzaes, *Angew. Chem., Int. Ed.*, 2005, **44**, 7852; (*d*) L. Durán Pachón and G. Rothenberg, *Appl. Organomet. Chem.*, 2008, **22**, 288; (*e*) H. Bönnemann

and R. M. Richards, *Eur. J. Inorg. Chem.*, 2001, 2455; (*f*) A. Roucoux, J. Schulz and H. Patin, *Chem. Rev.*, 2002, **102**, 3757; (*g*) J. D. Aiken III and R. G. Finke, *J. Mol. Catal. A: Chem.*, 1999, **145**, 1.

12 (*a*) K. T. Wu, Y. D. Yao, C. R. C. Wang, P. F. Chen and E. T. Yeh, *J. Appl. Phys.*, 1999, **85**, 5959; (*b*) E. W. Wong, M. J. Bronikowski, M. E. Hoenk, R. S. Kowalczyk and B. D. Hunt, *Chem. Mater.*, 2005, **17**, 237; (*c*) Y. W. Jun, Y. M. Huh, J. S. Choi, J. H. Lee, H. T. Song, S. Kim, S. Yoon, K. S. Kim, J. S. Shin, J. S. Suh and J. Cheon, *J. Am. Chem. Soc.*, 2005, **127**, 5732; (*d*) S. Mornet, S. Vasseur, F. Grasset and E. Duguet, *J. Mater. Chem.*, 2004, **14**, 2161; (*e*) F. Li, C. Vipulanandan and K. K. Mohanty, *Colloids Surf., A*, 2003, **223**, 103; (*f*) W. X. Zhang, *J. Nanopart. Res.*, 2003, **5**, 323; (*g*) D. Huber, *Small*, 2005, **1**, 482.

13 (*a*) R. B. Bedford, M. Betham, D. W. Bruce, S. A. Davis, R. M. Frost and M. Hird, *Chem. Commun.*, 2006, 1398; (*b*) Y. Moglie, E. Mascaró, F. Nador, C. Vitale and G. Radivoy, *Synth. Commun.*, 2008, **38**, 3861; (*c*) C. He, G. Tian, Z. Liu and S. Feng, *Org. Lett.*, 2010, **12**, 649; (*d*) See also ref. 11*g*.

14 P.-H. Phua, L. Lefort, J. A. F. Boogers, M. Tristany and J. G. de Vries, *Chem. Commun.*, 2009, 3747.

15 D. Farrell, S. A. Majetich and J. P. Wilcoxon, *J. Phys. Chem. B*, 2003, **107**, 11022.

16 O. Margeat, F. Dumestre, C. Amiens, B. Chaudret, P. Lecante and M. Respaud, *Prog. Solid State Chem.*, 2005, **33**, 71.

17 (*a*) H. Bönnemann, W. Brijoux, R. Brinkmann, R. Fretzen, T. Joussen, R. Koppler, B. Korall, P. Neiteler and J. Richter, *J. Mol. Catal.*, 1994, **86**, 129; (*b*) G. N. Glavee, K. J. Klabunde, C. M. Sorensen and G. C. Hadjipanayis, *Inorg. Chem.*, 1995, **34**, 28; (*c*) K. C. Huang and S. H. Ehrman, *Langmuir*, 2007, **23**, 1419.

18 Our high throughput experimentation setup is composed of a liquid handling robot (Zinsser Lissy: http://www.zinsser-analytic.com/Catalogue/exeProduct/?id=67) placed within a glovebox and a parallel hydrogenation reactor (Premex: http://www.premex-reactorag.ch/index.php?page=464) where up to 96 reactions can be carried out at the same time (Pressure max (100 bar H_2, 5 mL scale).

19 (*a*) Y. Takegami, T. Ueno and T. Fujii, *Bull. Chem. Soc. Jpn.*, 1966, **39**, 1; (*b*) A. R. Brodskii, V. F. Vozdvizhenskii, N. F. Noskova, A. S. Khlystov, O. M. Pakhorukova and D. V. Sokolskii, *J. Organomet. Chem.*, 1979, **178**, 325; (*c*) A. R. Brodskii, V. F. Vozdvizhenskii, N. F. Noskova, A. S. Khlystov, O. M. Pakhorukova and D. V. Sokolskii, *J. Organomet. Chem.*, 1979, **179**, 139.

20 (*a*) Y. Takegami, T. Ueno and T. Fujii, *Bull. Chem. Soc. Jpn.*, 1969, **42**, 11663; (*b*) W. R. Kroll and N. J. Linden, US patent 3 323 902, 1967; (*c*) California Research Corporation Patent 1 390 570, 1965.

21 (*a*) M. Kumada and J. K. Kochi, *J. Am. Chem. Soc.*, 1971, **93**, 1487; (*b*) J. K. Kochi, *Acc. Chem. Res.*, 1974, **7**, 351.

22 (*a*) R. S. Smith and J. K. Kochi, *J. Org. Chem.*, 1976, **41**, 502; (*b*) S. M. Neumann and J. K. Kochi, *J. Org. Chem.*, 1975, **40**, 599; (*c*) R. B. Allen, R. G. Lawler and H. R. Ward, *J. Am. Chem. Soc.*, 1973, **95**, 1692; (*d*) R. G. Lawler and P. Livant, *J. Am. Chem. Soc.*, 1976, **98**, 3710; (*e*) J. Kleimark, A. Hedström, P.-F. Larsson, C. Johansson and P.-O. Norrby, *ChemCatChem*, 2009, **1**, 152.

23 G. Cahiez, V. Habiak, C. Duplais and A. Moyeux, *Angew. Chem., Int. Ed.*, 2007, **46**, 4364.

24 A. Fürstner, R. Martin, H. Krause, G. Seidel, R. Goddard and C. W. Lehmann, *J. Am. Chem. Soc.*, 2008, **130**, 8773.

25 (*a*) B. Bogdanović and M. Schwickardi, *Angew. Chem., Int. Ed.*, 2000, **39**, 4610; (*b*) L. E. Aleandri, B. Bogdanović, P. Bons, C. Dürr, A. Gaidies, T. Hartwig, S. C. Huckett, M. Lagarden, U. Wilczok and R. A. Brand, *Chem. Mater.*, 1995, **7**, 1153; (*c*) G. Siedlaczek, M. Schwickardi, U. Kolb, B. Bogdanović and D. G. Blackmond, *Catal. Lett.*, 1998, **55**, 67.

26 We verified that the direct hydrogenation of 1-octene also follows a first order kinetic (see supplementary information†).

27 (*a*) G. Dazinger and K. Kirchner, *Organometallics*, 2004, **23**, 6281; (*b*) V. Guerchais, *J. Chem. Soc., Chem. Commun.*, 1990, 534; (*c*) M. Brookhart and W. B. Studabaker, *Chem. Rev.*, 1987, **87**, 411.

28 (*a*) A. Klose, J. Hesschenbrouck, E. Solari, M. Latronico, C. Floriani, N Re, A. Chiesi-Villa and C. Rizzoli, *J. Organomet. Chem.*, 1999, **591**, 45; (*b*) A. I. F. Venâncio, L. M. D. R. S. Martins and A. J. L. Pombeiro, *J. Organomet. Chem.*, 2003, **684**, 315; (*c*) G. Albertin, P. Agnoletto and S. Antoniutti, *Polyhedron*, 2002, **21**, 1755; (*d*) S. K. Russell, E. Lobkovsky and P. J. Chirik, *J. Am. Chem. Soc.*, 2009, **131**, 36.

29 A. Uzun and B. C. Gates, *Angew. Chem., Int. Ed.*, 2008, **47**, 9245.

30 (*a*) L. S. Ott and R. G. Finke, *Inorg. Chem.*, 2006, **45**, 8382; (*b*) L. S. Ott and R. G. Finke, *Coord. Chem. Rev.*, 2007, **251**, 1075.

31 B. D. Cullity and C. D. Graham in *Introduction to Magnetic Materials*, Wiley, John & Sons, Incorporated, 2009, pp.183.

32 (*a*) J. M. D. Coey, *Phys. Rev. Lett.*, 1971, **27**, 1140; (*b*) R. H. Kodama and A. E. Berkowitz, *Phys. Rev. B: Condens. Matter Mater. Phys.*, 1999, **59**, 6321; (*c*) J. Bansmann, S. H. Baker, C. Binns, J. A. Blackman, J.-P. Bucher, J. Dorantes-Dávila, V. Dupuis, L. Favre, D. Kechrakos, A. Kleibert, K.-H. Meiwes-Broer, G. M. Pastor, A. Perez, O. Toulemonde, K. N. Trohidou, J. Tuaillon and Y. Xie, *Surf. Sci. Rep.*, 2005, **56**, 189.

33 (*a*) I. M. L. Billas, J. A. Becker, A. Châtelain and W. A. de Heer, *Phys. Rev. Lett.*, 1993, **71**, 4067; (*b*) M. L. Tiago, Y. Zhou, M. M. G. Alemany, Y. Saad and J. R. Chelikowsky, *Phys. Rev. Lett.*, 2006, **97**, 147201.

34 F. Dumestre, B. Chaudret, C. Amiens, P. Renaud and P. Fejes,, *Science*, 2004, **303**, 821.

35 (*a*) J. L. Dormann, D. Fiorani and E. Tronc, *Adv. Chem. Phys.*, 1997, **98**, 283; (*b*) X. Batlle and A. Labarta, *J. Phys. D: Appl. Phys.*, 2002, **35**, R15; (*c*) R. Skomski, *J. Phys.: Condens. Matter*, 2003, **15**, R841.

36 C. de Julián Fernández, *Phys. Rev. B: Condens. Matter Mater. Phys.*, 2005, **72**, 054438.

37 J. A. Widegren and R. G. Finke, *J. Mol. Catal. A: Chem.*, 2003, **198**, 317.

38 G. M. Whitesides, M. Hackett, R. L. Brainard, J. P. P. M. Lavalleye, A. F. Sowinski, A. N. Izumi, S. S. Moore, D. W. Brown and E. M. Staudt, *Organometallics*, 1985, **4**, 1819.

39 F. Lihl, *Z. Metallk.*, 1953, **44**, 160.

40 A. F. Meindertsma, M. M. Pollard, B. L. Feringa, J. G. de Vries and A. J. Minnaard, *Tetrahedron: Asymmetry*, 2007, **18**, 2849.

41 J. Garcia-Antón, M. Rosa Axet, S. Jansat, K. Philippot, B. Chaudret, T. Pery, G. Buntkowsky and H-. H. Limbach, *Angew. Chem., Int. Ed.*, 2008, **47**, 2074.